Rapid pH Change due to Bacteriorhodopsin Measured with a Tin-Oxide Electrode

Baldwin Robertson and Evgeniy P. Lukashev
Biotechnology Division, National Institute of Standards and Technology, Gaithersburg, Maryland USA

ABSTRACT The photocurrent transient generated by bacteriorhodopsin (bR) on a tin-oxide electrode is due to pH change and not to charge displacement as previously assumed. Films of either randomly oriented or highly oriented purple membranes were deposited on transparent electrodes made of tin-oxide-coated glass. The membranes contained either wild-type or D96N-mutant bR. When excited with yellow light through the glass, the bR pumps protons across the membrane. The result is a rapid local pH change as well as a charge displacement. Experiments with these films show that it is the pH change rather than the displacement that produces the current transient. The calibration for the transient pH measurement is given. The sensitivity of a tin-oxide electrode to a transient pH change is very much larger than its sensitivity to a steady-state pH change.

INTRODUCTION

Bacteriorhodopsin (bR) is a protein-chromophore complex that gives the color to the purple membrane from *Halobacterium salinarium* (formerly *Halobacterium halobium*). When bR absorbs yellow light, it pumps protons across the membrane (Oesterhelt and Stoeckenius, 1971). Retinal, the chromophore that is bound to Lys-216 of the protein by a protonated Schiff base, is responsible for the absorption, which occurs at about 570 nm. A quantum of yellow light induces a *trans-cis* isomerization of retinal followed by transitions of the complex through a number of intermediate states, back to the ground state bR. These intermediates have different absorption spectra, different life times (from subpico- to milliseconds), and different protonation states of the Schiff base and of several amino acids (Ebrey, 1993; Lanyi, 1993; Mathies et al., 1991).

The M intermediate is formed when the proton on the Schiff base is transferred to Asp-85, and subsequently a proton from an unknown amino acid XH (possibly Arg-82) is released into the periplasmic solution (Balashov et al., 1993). When the M state decays, the Schiff base is reprotonated from Asp-96. This was shown with the D96N mutant, in which a nonprotonable asparagine replaces the protonable aspartate in the 96 position. The substitution makes the M-decay rate much slower (Miller and Oesterhelt, 1990; Butt et al., 1989), more so at high pH (Holz et al., 1989; Tittor et al., 1989). This shows that in the mutant the Schiff base is reprotonated from the solution, and that in the wild type it is reprotonated from Asp-96. Then, continuing the cycle for wild-type bR, a proton from the cytoplasmic solution reprotonates Asp-96, and retinal reisomerizes back to the all-*trans* configuration. Finally, the proton from Asp-85 reprotonates the proton release group X^-, returning bR to its initial state (Ebrey, 1993; Mathies et al., 1991; Lanyi, 1993).

This order of deprotonation and reprotonation events (and the proton release before proton uptake) occurs at neutral and high pH. At low pH, the sequence of deprotonation and reprotonation events is different, and proton uptake can occur before release (Garty et al., 1977; Takeuchi et al., 1981). For pH above 5, there is net proton release by bR to the periplasmic solution, and for pH below 4, there is net proton uptake by bR from the cytoplasmic solution (Dencher and Wilms, 1975; Zimanyi, 1992).

Measurements of the light-induced transient current produced by bR have been reported (Miyasaka and Koyama, 1991; Miyasaka and Koyama, 1992; Miyasaka et al., 1992). The current was produced by a purple-membrane film deposited on a semitransparent electrode made of tin-oxide-coated glass immersed in an aqueous solution. Recently a charge-displacement model for the origin of the transient current has been proposed (Koyama et al., 1994). We will describe a different model in which the proton release and uptake by bR causes a pH change that the tin oxide converts into an electrochemical current. We report experiments intended to distinguish between these models and to help understand the cause of the current.

Tin-oxide electrodes with dried purple-membrane films have been widely used in studies of photopotentials produced by bR in air (Varo 1981; Kononenko et al., 1987; Groma et al., 1988; McIntosh and Boucher, 1991; Haronian and Lewis, 1991). Tin oxide may be the best semiconductor for this purpose since its large forbidden gap (≈3.7 eV) is not excited by visible light (Kim and Laitinen, 1975). Metal-oxide electrodes have an electrochemical equilibrium potential that depends on pH, and tin-oxide electrodes are not an exception. At low salt concentrations, the dependence is linear, although the slope depends on the history of the electrode. For a new tin-oxide electrode kept in distilled water, the slope is −37 mV/pH unit, and after the electrode is soaked in 10 M NaOH, the slope increases in magnitude to −59 mV/pH unit (Laitinen and Hseu, 1979). A slope of −46.6 mV/pH unit has also been reported (Fog and Buck,

Received for publication 12 September 1994 and in final form 23 December 1994.

Address reprint requests to Dr. Baldwin Robertson, A353 Chem, National Institute of Standards and Technology, Gaithersburg, MD 20899. Tel.: 301-974-5948; Fax: 301-330-3447; E-mail: baldwin@nist.gov.

0006-3495/95/04/1507/11 $2.00

1984). Although tin and its oxides have complicated equilibrium potential-pH phase diagrams in water (Deltombe et al., 1966; Galus, 1975), tin-oxide electrodes are widely used because of their mechanical stability, their optical transparency, and their lack of a current or voltage response to visible light (Jarzebski and Marton, 1976).

In this paper we present evidence that shining yellow light on a purple-membrane film on a tin-oxide electrode produces an electrochemical current that is a measure of the local pH change at the electrode surface caused by bR. The effect is due to a redox reaction accompanying the change in proton concentration at the electrode surface and not to the electric charge displacement produced by proton transfer from one side of the membrane to the other. We demonstrate the feasibility of using a tin-oxide electrode for observing fast transient pH changes created by bR.

MATERIALS AND METHODS

Purple membranes were purified from wild-type or D96N-mutant *H. salinarium* (Soppa and Oesterhelt, 1989) as described by Becher and Cassim (1975). The sample was centrifuged five additional times in deionized water to obtain a suspension of purple membrane patches with very low ionic conductivity.

The working electrode was a 25 × 25 × 3.2 mm soda-lime glass slide coated on one surface with a roughly 500 nm-thick transparent antimony-doped tin-oxide conducting layer (Delta Technologies CG-100SN). (Note: Commercial names of materials and apparatus are identified only to specify the experimental procedure. This does not imply a recommendation, nor does it imply that they are the best available for the purpose.) The glass was coated in 1981 using a continuous process. Large sheets of glass were heated in air to 425° or slightly hotter, but below the flow point. Then a solution of anhydrous $SnCl_2$ and $SbCl_3$ in absolute isopropanol was sprayed onto the glass, forming an $Sn_xSb_yO_z$ vitreous coating (L-O-F Liberty Mirror, Electropane). The resistance of the slides measured between two probe tips touching the surface 1 cm apart varied from 170 Ω to 325 Ω, with an average value of about 200 Ω.

A new electrode was washed in acetone and ethanol and rinsed in deionized water. Then 25 μl of a suspension of purple membrane having a bR concentration of 5–6 mg/ml was pipetted onto about 1 cm^2 of the electrode surface, and the electrode was dried in a closed Petri dish at room temperature and humidity. This concentration was used for most experiments. For one thin-layer experiment, 0.5 mg/ml was used. For another experiment, highly oriented films of wild-type and D96N-bR were electrophoretically sedimented onto the slide following a procedure (Varo, 1981) used previously for making dry films (Kononenko et al., 1987).

The absorption spectrum of the purple membrane film on the tin-oxide glass slide was measured using a diode-array spectrophotometer (Hewlett Packard 8452A).

The coated glass electrode was placed coating-up at the bottom of an electrochemical cell. Leaks between the glass and the sides of the cell are prevented by a rubber O-ring (1 cm inside diameter, 1 mm diameter) compressed between the glass and the bottom of a thick tube used for the sides of the cell. The tube is made of black nylon (Delrin) and has a 6-mm inside diameter. A saturated Ag/AgCl electrode (Microelectrodes MI-401) was used for the reference electrode; its tip was positioned 1.5 cm above the working electrode, and the free surface of the electrolyte was 1.5 cm above that. The counter electrode was a 0.2 mm platinum wire wrapped 6 times around the 1-mm glass barrel of the reference electrode. The cell holds 1 ml of electrolyte.

An electrochemical interface (Solartron 1286) was used with its standard resistance set to 10^4 Ω in potentiostatic mode for current measurements, and in galvanostatic mode for equilibrium potential measurements. The direct-coupled current output signal was connected to an 8-pole low-pass filter (Frequency Devices 902) set to 100 Hz corner frequency, and the filtered transient signal was recorded with a digital signal processor (Stanford Research Systems 850) with a direct-coupled input. The overall current gain was calibrated, with the dc ammeter on the interface as a standard, by changing the controlled potential, waiting for the recorded output to settle, and dividing the change in the ammeter indication by the change in the recorded output. Because of the direct coupling, this calibration for changes in the steady-state is valid also for transients.

The response time of the system in the potentiostatic mode was measured by stepping the potential from 0 mV to −1 mV. This induces a cathodic current transient (without bR on the electrode) with a rise time of 4 ms and decay time of 20 ms. A step in the opposite direction produced an anodic spike of the same shape and the same time constants. The decay time decreased with increasing concentration of supporting ions and reached a constant at concentrations higher then 100 mM KCl. The 4-ms rise time is the response time of the system.

The light source was a 300-W halogen lamp in a slide projector (Kodak) with a lens that produced a horizontal light beam. The projector was kept 30 cm from the electrochemical cell to reduce heating and electrical interference, and the light beam was directed vertically upward by a mirror underneath the cell. The light was filtered with, in sequence, a water filter (Oriel 71260), a heat-absorbing filter (Oriel 59060) and long-pass, band-pass, or interference filters, and was focused up through the glass electrode onto the purple-membrane film with a 38-mm diameter F/2 borosilicate crown glass lens (Oriel 40550). A yellow long-pass (530 nm) filter (Oriel 59500) was used for activating bR in its absorbance band. A blue band-pass (298 nm to 435 nm) filter (Oriel 59814) was used for activating the M intermediate in its absorbance band. The light was controlled with an electric shutter (Melles Griot 04 IES 001) actuated electronically (Melles Griot 04 ISC 001) with a full-scale slew time of about 3 ms. The maximum incident power of yellow light at the sample was 20 mW/cm^2, and that of blue light was 1.5 mW/cm^2, as measured with a laser radiometer (Aerotech 71). The action spectrum of the photocurrent or photovoltage was measured with a set of interference filters (Oriel 54161) with centers every 20 nm from 480 to 640 nm, each filter having 10 nm bandwidth. An inconel-coated quartz neutral-density filter (Corion) with an optical density of 1.0 was used to reduce the light intensity for one experiment.

All experiments were conducted at room temperature using a new tin-oxide electrode with 1 ml of 100 mM KCl and a variety of buffers in deionized water as the electrolyte, which was exposed to air. All chemicals (salts, buffers, solvents) were analytical grade from Aldrich, Sigma, and Fluka.

A thick purple-membrane film on the electrode had to be soaked for an hour in the electrolyte solution in the electrochemical cell in order to make the transient photocurrent repeatable. A thin film required only a few minutes. Without the bR film on the tin-oxide electrode there is no measurable photocurrent due to visible light at the intensity used in the experiments, in agreement with previous studies (Kim and Laitinen, 1975).

RESULTS

Peak photocurrent

The amplitude of the peak of the photocurrent transient reflects the properties of bR. A film of randomly oriented multiple layers of purple-membrane patches was deposited on a transparent electrode made of tin-oxide-coated glass, a supporting electrolyte was added, and the electrode was connected to an electrochemical interface in the potentiostatic mode. The potential was set so that the current was approximately zero (less than a few nanoamperes). When the film is illuminated with yellow light, a transient current results, an example of which is in the upper left of Fig. 1. No photocurrent is observed (to an accuracy of 1 nA) in the absence

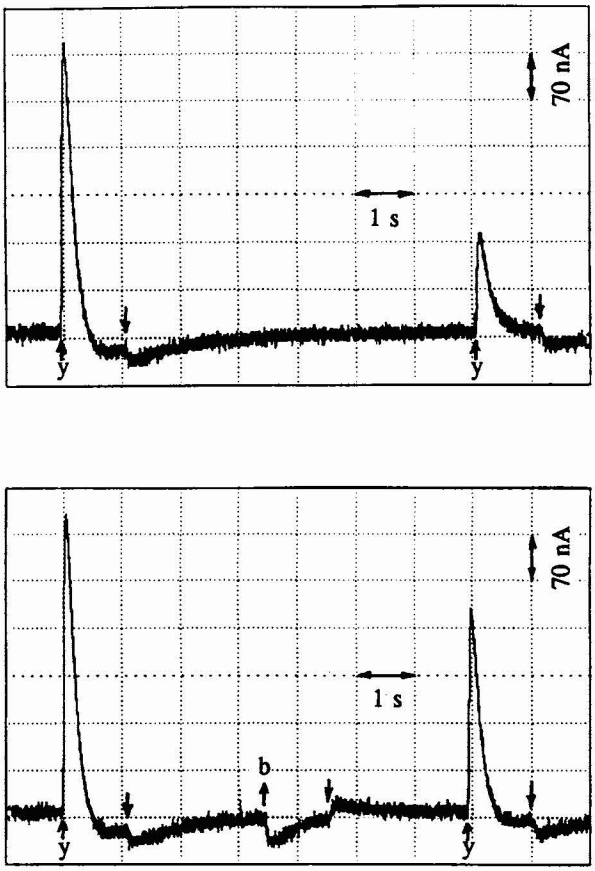

FIGURE 1 Time dependence of the transient current generated by 1-s flashes of yellow (y) and blue (b) light on a film of randomly oriented D96N purple-membrane patches on a tin-oxide electrode. The up and down arrows denote light on and off, respectively. Yellow light intensity: 20 mW/cm^2. Blue light intensity: 1.5 mW/cm^2. Potential: 0 mV. Electrolyte: 100 mM KCl, 10 mM sodium borate buffer, pH 9.

of bR. The amplitude and shape of the photocurrent transient in the presence of bR are highly repeatable as long as the experimental conditions are not changed. We will show that the magnitude of the peak current is determined by the bR in the film.

The amplitude of the current pulse increases with the amount of the M-state intermediate produced by the light. This can be seen from the upper curve of Fig. 1, which is a current pulse due to a 1-s flash of yellow light on a D96N film, followed 7 s later by a current pulse due to another flash. The first flash converts a number of molecules to the M state, thus reducing the population of the bR ground state available for generating the second current transient.

If the delay between flashes is much shorter than the turnover time of the photocycle, the second current peak is much smaller than the first. The larger the separation between flashes, the larger the second peak. A plot of the amplitude of the second peak versus the delay time permits calculating the half-time of the M decay, which is 8 s at pH 9.0. The M state can also be observed by measuring its optical absorbance at 412 nm (Ebrey, 1993; Mathies et al., 1991). The half-time calculated from the photocurrent agrees with the half-time calculated from the light-induced change of absorbance of bR in the same electrolyte.

An intervening flash of blue light replenishes the population of bR available for generating the current pulse due to the second flash of yellow light as in the lower curve in Fig. 1. The replenishment occurs because illuminating the M intermediate in its absorbance band at 412 nm accelerates the M-to-bR back reaction (Karvaly and Dancshazy, 1977; Druckmann et al. 1992). Even though the blue light is only 1/15 as intense as the yellow light, it more than doubles the second yellow peak.

Comparison of the action spectrum of the light-induced transient current with the optical absorbance spectrum of bR provides the most convincing evidence that the peak current is generated by bR. The action spectrum is the magnitude of the peak current that results from shining light through a narrow-pass filter onto the purple membrane patches, versus the wavelength of light passed by the filter. The maximum transmittance of the narrow-pass filters is nearly constant from 480 to 640 nm, and the light source intensity increases smoothly in this interval, without a peak. In Fig. 2 the action spectrum for a D96N film at pH 7 (filled circles) is compared with the optical absorbance (solid curve) of the same film in the same solution. The agreement of the two spectral peaks shows that the peak photocurrent transient is due to bR.

When the light intensity is decreased, the magnitude of the peak current decreases, and the shape of the transient changes, as in Fig. 3 for the D96N mutant. The peak current is 250 nA for light of 20 mW/cm^2 intensity (upper curve), and is 50 nA for 2 mW/cm^2 (lower curve). The time constant for the light-on phase of the transient also depends strongly on the intensity of the exciting light; it is longer at lower intensity than at higher intensity. The shape of the off phase depends only slightly on the intensity that the light had when it was on. Similar results are observed for the optical absorbance at 412 nm of the same film in the same solution. This suggests that the on phase of the photocurrent transient corresponds mostly to the accumulation of the M intermediate, while the off phase corresponds to M decay—at least for the D96N mutant at pH 7, which has an M-decay rate that is slow enough to see on this time scale.

A purple-membrane film that is dark adapted by keeping it overnight in the electrochemical cell in the dark, when first illuminated with yellow light, has a photocurrent whose amplitude is approximately one half that for the same film after it is adapted to yellow light and then reset with blue light. This is explained as follows. The chromophore of dark-adapted bR is ½ *trans* and ½ *cis*, while the chromophore of light-adapted and reset bR is entirely *trans*. Only the *trans* bR produces the M intermediate, which accompanies proton release (Ebrey, 1993).

All these examples of the behavior of the amplitudes of the photocurrent pulses reflect well-known properties of bR and establish that the amplitude of the peak current through the

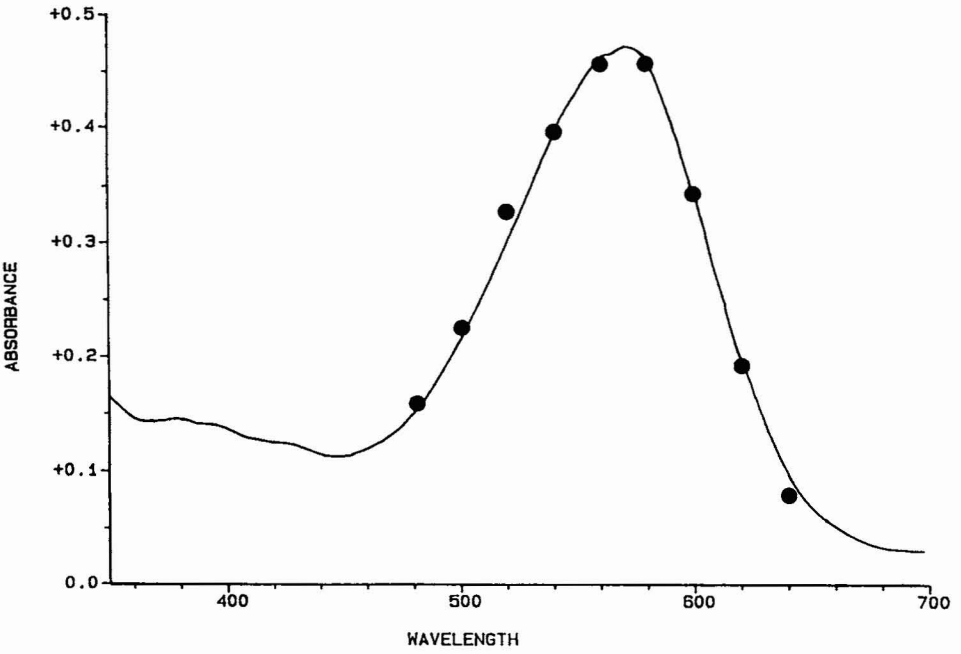

FIGURE 2 Action spectrum of the peak current due to a randomly oriented D96N film (●), compared with the optical absorbance (*solid curve*) of the same film in the same solution. The current has been normalized to the maximum absorbance. Potential: 0 mV. Electrolyte: 100 mM KCl, 10 mM phosphate buffer, pH 7.

tin-oxide electrode is proportional to the number of bR molecules in the ground state.

Effect of bacteriorhodopsin

The light-induced release by bR of protons onto the periplasmic side of the membrane and the subsequent uptake of protons from the cytoplasmic side results in two physical phenomena: 1) the charge displacement that accompanies translocation of protons across the membrane generates an electric potential difference across the membrane; and 2) the release of protons lowers the pH of the solution on the periplasmic side, and the uptake of protons raises the pH on the cytoplasmic side. Either of these phenomena could result in an electrical signal. We will show that the first is not the primary cause of the observed photocurrent and that the second does provide a consistent explanation of what is observed.

The production of the photocurrent from randomly oriented D96N films is largely a surface effect rather than a volume effect. This can be deduced from Fig. 4. The absorbance at 560 nm of the film that generated the upper transient in this figure was 0.45, while that for the lower transient was 0.045. The film thicknesses that correspond to these optical densities are roughly 200 and 20 patches thick, respectively (Miyasaka and Koyama, 1992). Even though the film for the upper curve is 10 times thicker than that for the lower one, the amplitude, and to a large extent the shape, of the curves are roughly the same. The only noticeable differences are that the lower transient has a small undershoot, while the upper one does not, and also the subsequent light-off transients are somewhat different. Both are relatively small differences. The substantial similarity of the two curves suggests that just the first purple-membrane layer in contact with the tin-oxide electrode causes most of what is observed. The remaining layers on the outside serve only to modify the shape of the transient slightly.

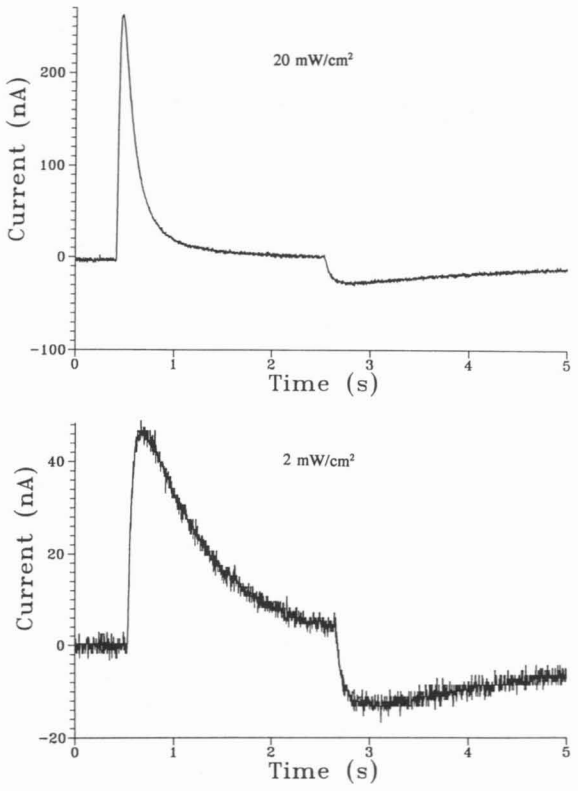

FIGURE 3 Photocurrent versus time produced by a randomly oriented D96N film in yellow light of intensity 20 mW/cm² (*upper curve*) and 2 mW/cm² (*lower curve*). The first spike occurs when the yellow light is turned on; the second (negative) transient occurs when the light is turned off ~2 s later. Potential: 0 mV. Electrolyte: 100 mM KCl, 10 mM phosphate buffer, pH 7.

Highly oriented thick films, on the other hand, may be expected to produce a volume effect rather than a surface effect. The nearly identical orientation of the purple-

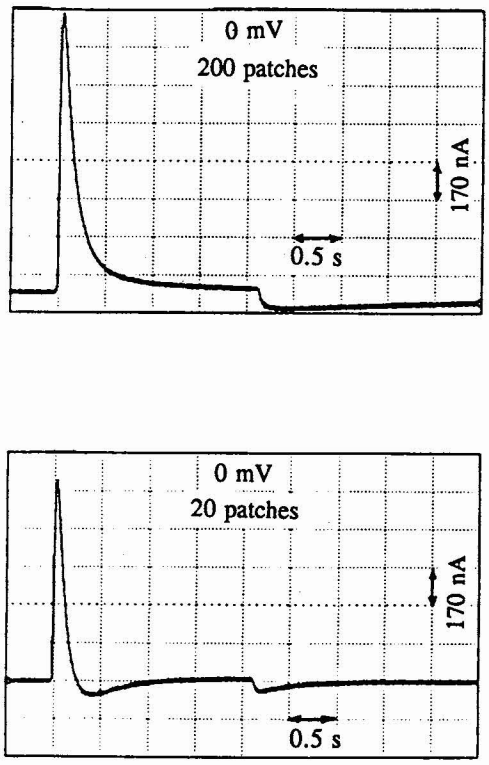

FIGURE 4 Effect of film thickness on the time dependence of the photocurrent produced by randomly oriented D96N films. Films with optical absorbance 0.45 are about 200 purple-membrane patches thick (*upper curve*), and those with absorbance 0.045 are 20 patches thick (*lower curve*). The first spike occurs when 20 mW/cm^2 of yellow light is turned on; the second transient occurs 2 s later when the light is turned off. Potential: 0 mV. Electrolyte: 100 mM KCl, 10 mM sodium phosphate buffer, pH 7.

membrane patches in the film will cause the photopotentials produced by the proton translocation in successive layers to accumulate and produce a more easily measurable total voltage.

D96N-mutant patches were electrophoretically sedimented to form a film on a tin-oxide electrode using a procedure described by Kononenko et al. (1987). This orients the purple-membrane patches predominantly with their cytoplasmic side toward the electrode. The cytoplasmic side is charged more negatively and so is more strongly attracted to the electrode, which served as the anode during the electrodeposition. Before the film was put into the cell, its photopotential was measured. At room humidity (RH <0.4), yellow light generates several volts across the film due to proton displacement toward the extracellular side of the membrane. Thus our film of highly oriented patches had a rather large accumulation of membrane-potential differences.

However, in the electrochemical cell at pH 7, the film of highly oriented D96N patches generated a photocurrent whose amplitude is only one half of that generated by a film of randomly oriented D96N patches (data not shown). Films with highly oriented patches generate a much larger total voltage than films with randomly oriented patches, but the observed current was not larger. Therefore the accumulated-potential model does not explain the photocurrent, although at the present we can not tell whether this effect contributes small corrections.

We now describe the results of experiments to test the model that light causes bR to produce a pH change, which causes the transient photocurrent.

Films of randomly oriented wild-type bR generate a photocurrent of small amplitude compared with that for randomly oriented D96N as in Fig. 5. This occurs because the turnover rate of the wild type is short compared with the time scale of the transient. Thus the wild-type patches with their cytoplasmic side next to the electrode can quickly take up protons from the solution that is between themselves and the electrode. At the same time, patches oriented the other way release protons into the solution between themselves and the electrode. Patches that release protons near the electrode generate an electrochemical current in one direction, and patches that take up protons near the electrode generate current in the other direction. The two currents cancel somewhat, and the total current is smaller than either component.

Films with randomly oriented D96N patches at neutral or high pH only release protons next to the electrode surface. Uptake of protons essentially does not occur because the proton concentration in solution is low, and the proton from solution must diffuse to the Schiff base to bind. The time required for this is the decay time of the M state, which is longer than the time the light is on. Thus the current produced by proton release is not cancelled by proton uptake, as occurs with the wild type. Therefore, films with randomly oriented D96N patches produce the largest photocurrent, which is what we observe.

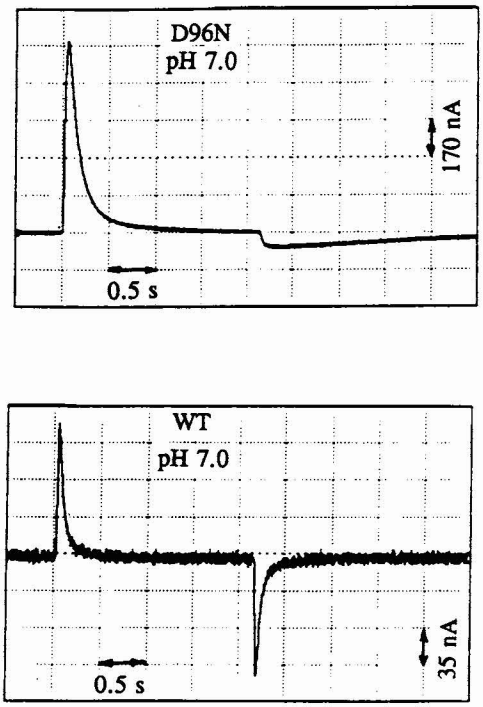

FIGURE 5 Photocurrent versus time for a randomly oriented film of D96N (*upper curve*) and wild-type (*lower curve*) bR at pH 7. The light is the same as in Fig. 4. Potential: O mV. Electrolyte: 100 mM KCl with 10 mM sodium phosphate buffer.

Films with highly oriented wild-type patches generate a photocurrent in the opposite direction from the photocurrents generated by films with randomly oriented patches at neutral or high pH (data not shown). This occurs because most of the oriented patches are oriented with their cytoplasmic side toward the electrode and hence can only uptake protons from the solution between themselves and the electrode.

One may conclude that the measurements of the peak photocurrent are consistent with predictions based on the pH change due to proton release and uptake by bR, and are not consistent with predictions based on the electric charge displacement generated by bR.

Electrode reaction

The photocurrent is an electrochemical current, which involves a redox reaction at the tin-oxide electrode. This can be seen by considering the plateau in the photocurrent that follows the decay from the peak in the upper curve of Fig. 6. Even if the yellow light is left on for well over 1 min, the current remains constant. This steady current can occur only if there is a redox reaction at the electrode surface. This conclusion can be extended: the entire photocurrent transient is, at least in part, the result of a chemical reaction at the electrode.

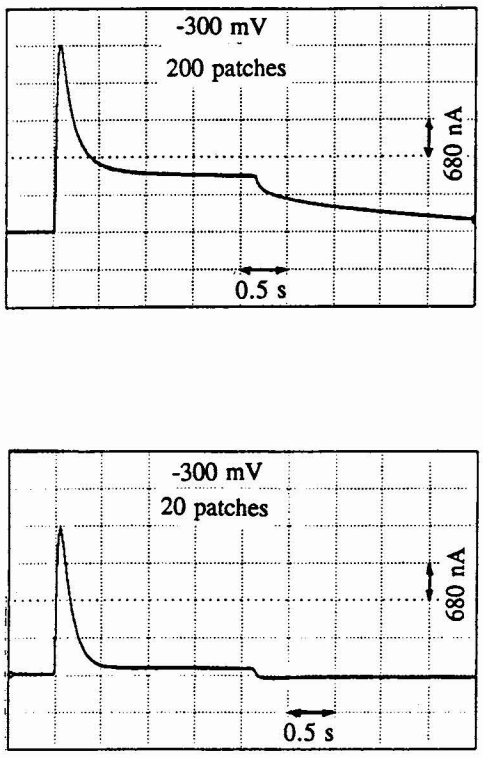

FIGURE 6 Effect of film thickness and voltage on the time dependence of the photocurrent produced by randomly oriented D96N purple-membrane films. Compare with Fig. 4. The films here as in Fig. 4 are about 200 purple-membrane patches thick (*upper curve*) and 20 patches thick (*lower curve*). Potential: −300 mV. Electrolyte: 100 mM KCl, 10 mM sodium phosphate buffer, pH 7.

The reaction involves protons, as can be seen by considering the equilibrium potential, which depends on pH as in Fig. 7. The potential measurements of the bare tin-oxide electrode were made in galvanostatic mode at zero current with continuous stirring. The time to reach a new equilibrium potential depends strongly on pH. In the alkaline region, after the electrolyte is replaced with one at another pH, 30 min are required to reach a constant potential, while in the acid region, 5 min are sufficient. The three curves are for three chloride concentrations. The uppermost curve is for 1 M KCl, the middle line is for 10 mM KCl, and the lowest line is for zero concentration. The two straight lines have a slope of −37 mV/pH unit, in agreement with Laitinen and Hseu (1979). Each scan was made from pH 9 to pH 2. The hysteresis on scanning back to pH 9 was less then 30 mV on average. Thus the data in Fig. 7 for each chloride concentration are a reasonable approximation to the equilibrium potential as a function of pH. The dependence on pH, or equivalently on the proton concentration, arises because protons bind and dissociate at the electrode.

Protons are also involved in transient currents. As described in Materials and Methods, a −1 mV step generates a current transient that is almost identical to the lower curve in Fig. 5, except that here there is no bR on the electrode. The values of the peak of this transient versus pH are the data points in Fig. 8. Here the amplitude of the peak current is a constant 400 nA (independent of pH) plus a term that increases exponentially to a total of 950 nA as the pH of the electrolyte is decreased to 3. The total at any pH includes the current that charges the double-layer capacitance when the voltage across it is changed, plus current due to the reaction at the electrode. Although the magnitude of the current

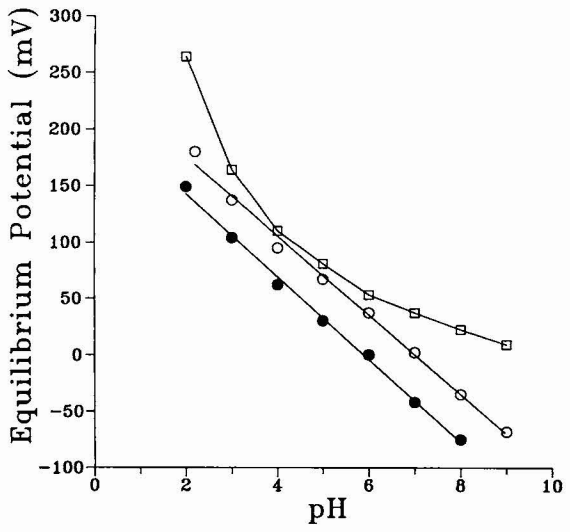

FIGURE 7 pH dependence of the equilibrium potential of a new tin-oxide electrode with a Ag/AgCl reference electrode. Electrolyte: 1 M KCl (*upper curve*), 10 mM KCl (*middle line*), and 0 mM KCl (*lower line*), each with 10 mM potassium borate buffer and boric acid for pH 9; or with 10 mM of phosphoric acid and potassium phosphate buffer for pH 8, 7, and 2; or with citric acid and potassium citrate buffer for pH 6, 5, 4, and 3. No HCl was used to adjust pH, so the chloride ion concentration is near zero for the lower line.

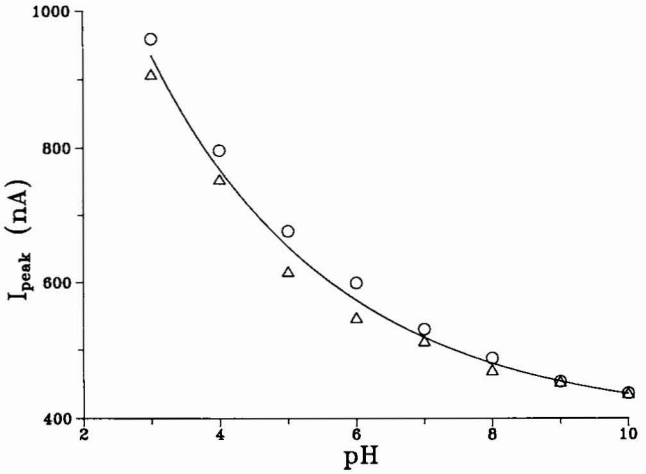

FIGURE 8 Peak value of the transient current that results from a −1 mV step on a tin-oxide electrode without a bR film. The measurements were made incrementing pH from 3 to 10 (*circles*) and then from 10 to 3 (*triangles*). The curve is the function $I_{peak} = A \cdot 10^{-k\,pH} + B$ fit to the data, where the fit values are $A = 1632$ nA, $B = 395$ nA, and $k = 0.160$. Initial potential: 0 mV. Electrolyte: 1 M KCl with a mixture of buffers consisting of 100 mM sodium citrate, 100 mM sodium phosphate, and 100 mM borate, titrated with HCl or NaOH to adjust pH.

peak depends on salt concentration (as mentioned in the Materials and Methods section), it does not depend on buffer concentration. The pH dependence of this current peak is the most important property here. It shows that protons must participate in the electrode reaction during the current transient.

When protons from solution participate in a reaction, the rate will depend on the proton concentration. We conclude that the magnitude of the peak photocurrent in potentiostatic mode is a measure of the local pH change at the electrode surface.

pH-current calibration

Before we understood the cause of the photocurrent, we attempted to calibrate the current change caused by a pH change using the following procedure. The potential was set to the equilibrium value for the electrolyte at a given pH. The pH of the electrolyte was changed, and the current was allowed to settle and then measured. When the pH was reduced by one unit, the steady current was ~25 nA cathodic; when the pH was increased one unit, the current was ~25 nA anodic. These measurements were done without the bR film on the electrode, both in zero salt concentration, and in 100 mM KCl, with the same results. With this calibration, the transient in Fig. 4 has a peak pH change of 51 units, which is obviously not reasonable. We describe this attempted calibration only to make it clear that it is not applicable.

The enormous number of pH units is not a result of how the apparatus was connected. We rechecked the sensitivity of the measuring system for both steady-state changes and transient changes, i.e., the dc and ac gains. We compared our results with those obtained using an electrochemical interface made by a different manufacturer, and with those using fast chart recorders in place of the digital signal processor. We are confident that the calibration described in the Materials and Methods section is correct for transient as well as steady-state changes.

The correct calibration of the current produced by a transient local pH change can be made by observing that changing the proton concentration changes the equilibrium point. A pH change of −1/37 unit produces a change in the equilibrium potential of +1 mV, which follows from Fig. 7. Because the photocurrent measurements are made with the interface in the potentiostatic mode, the actual potential difference between the working and reference electrodes does not change. The change in equilibrium point produces the same effect as a change in applied potential of the same magnitude but opposite sign. The result is a current transient whose peak value ranges from 400 to 950 nA depending on pH as in Fig. 8. The current peak in Fig. 4, for example, is generated by a pH change of roughly −2/37 unit. In general, the correct calibration of the current produced by a transient local pH change is obtained in a similar way from Figs. 7 and 8.

The enormous difference between the sensitivity for steady-state measurements and that for transient measurements is a property of the electrochemistry at the electrode. This can be seen by studying the current transient that results from a voltage step. Close examination reveals that following the large current spike there is a very small steady-current plateau. It is the tiny plateau that gets measured in a steady-state measurement, but it is the large spike that is observed in the transient measurement. Recall that the large spike includes not only the current that charges the double-layer capacitance, but also a pH-dependent term that is the result of a redox reaction at the electrode. The enormous difference in sensitivity between transient and steady-state changes applies, not only to potential changes at constant pH, but also to pH changes at constant potential.

Proton release and uptake

At low pH the photocurrents of both D96N and wild-type randomly oriented bR films are in the opposite direction from those at neutral pH as in Fig. 9. The reversal of the current occurs because there is net uptake of protons by bR. The reverse current is due to well-known properties of bR (Ebrey, 1993; Lanyi, 1993) and is not an artifact of the tin-oxide electrode, as we will discuss.

The dependence of the peak photocurrent on pH is given in Fig. 10 for films of randomly oriented D96N (upper curve) and wild-type (lower curve) bR. We begin the explanation of the shape of this curve at pH 7. As mentioned in the introduction, at neutral pH a proton is released into the periplasmic solution during the formation of the M state. This generates a cathodic current, which is the maximum. As the pH is decreased below 7, the peak photocurrent changes sign where net proton release changes to net proton uptake (Garty et al., 1977; Takeuchi et al., 1981; Varo and Lanyi,

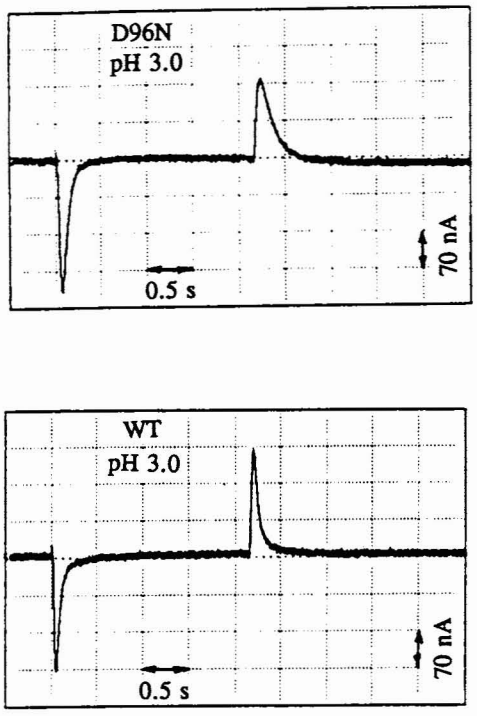

FIGURE 9 Photocurrent versus time for a randomly oriented film of D96N (*upper curve*) and wild-type (*lower curve*) bR at pH 3. The effect of pH can be seen by comparing with Fig. 5. Potential: O mV. Electrolyte: 100 mM KCl with 10 mM sodium citrate buffer.

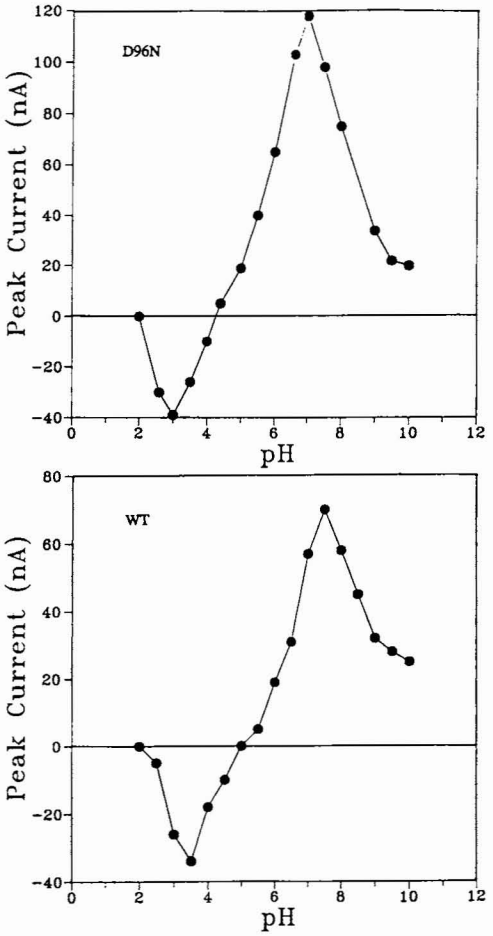

FIGURE 10 pH-dependence of the peak photocurrent for D96N (*upper curve*) and wild-type (*lower curve*) purple-membrane films, both at 0 mV. Electrolyte: 100 mM KCl with a mixture of buffers consisting of 10 mM sodium citrate, 10 mM sodium phosphate, and 10 mM sodium borate, titrated with HCl or NaOH to adjust pH.

1990). For D96N-mutant and wild-type bR, the sign change occurs at pH 4.5 and 4.0, respectively. Cathodic photocurrent corresponds to net proton release, anodic to net proton uptake.

The decrease in the photocurrent as the pH is increased above 7 is explained as follows. The proton is released from an unknown group XH (possibly Arg-82), which has a pK of 8.2 in the ground state of bR (Kono et al., 1993). This means that as the pH is increased in this range, the XH group becomes more likely to be already deprotonated before the light flash. When XH is already deprotonated, the light-induced response of bR can not cause it to release a proton into solution and contribute to the photocurrent.

As the pH is decreased below 3, Asp-85 becomes more likely to be already protonated before the photocycle is initiated, since the pK for proton binding to Asp-85 is 2.5 (Ebrey, 1993; Lanyi, 1993). As a result the membrane is blue, and the proton can not transfer to Asp-85 from the Schiff base. Later in the photocycle, since the Schiff base is still protonated, it can not receive the proton from Asp-96, which as a result can not uptake a proton from solution. This explains the decrease in magnitude of the peak photocurrent as the pH is decreased below 3.

The reversal of the sign of the photocurrent transient, along with the behavior at extreme values of pH, are reflections of the well-known properties of bR and are not particular to tin-oxide electrodes.

The sign of the blue-light-activated current in Fig. 1 is also opposite to the yellow-activated current. This shows that there is proton uptake in the back reaction of M to bR. Our experiments do not indicate which side of the membrane takes up the proton. But a recent study showed that in this reaction the Schiff base is reprotonated from the primary acceptor, Asp-85 (Druckmann et al., 1992). This residue is on the periplasmic side of the purple membrane, so the uptake must have occurred on that side.

Further experiments

The presence of buffer reduces the amplitude of the peak of the photocurrent transient as in Table 1. These measurements were made with a D96N film in 100 mM KCl electrolyte with sodium phosphate buffer of the indicated concentration at pH 7 at a potential of 0 mV. As the buffer concentration is increased from 0 to 1 mM, the magnitude of the peak photocurrent increases, and the steady-state photocurrent, although small, is noticeable, as in the upper curve of Fig. 11. At intermediate buffer concentration (5–10 mM), the magnitude levels off, the rise and relaxation of the photocurrent are faster, and the steady-state photocurrent decreases. As the

TABLE 1 Effect of buffer concentration on peak photocurrent

Concentration (mM)	Current (nA)
0.0	205
0.1	295
1	650
10	907
25	634
50	428
100	226

buffer concentration is increased above 10 mM, the peak photocurrent decreases strongly, the decay rate increases, and an undershoot occurs in the decay as in the lower curve in Fig. 11. These effects of buffer concentration must be taken into account in assessing the ability of an injection of protons by bR to produce a current peak.

A new tin-oxide electrode is hydrophobic and is transparent with a slight tint due to optical interference. After a microampere or more of current has flowed for a few minutes or more, the tin-oxide film becomes hydrophilic and gray, which is evidence that the properties of the electrode have changed. The change occurs during measurements of the steady-state current-voltage relationship of the tin-oxide electrode. The current-induced change must be taken into account in order to obtain repeatable results.

The magnitudes of the peak photocurrent, the steady photocurrent plateau, the step-voltage-induced peak current, and the dark current all seem to have terms that depend on the applied potential and the pH in approximately the same way. These terms appear roughly to satisfy the usual current-potential equation, which has an exponential dependence on overpotential (Bard and Faulkner, 1980; Oldham and Myland, 1994).

The steady photocurrent plateau occurs only for a thick film of D96N bR at neutral or high pH and low buffer concentration and large negative potential. The plateau does not occur for wild-type bR. The thicker the purple-membrane film, the larger the plateau (Fig. 6). For a thin film, the transient photocurrent has an undershoot (lower curve of Fig. 4). Even for a thick film at a large negative potential, the plateau completely vanishes at higher buffer concentrations and is replaced by an undershoot (Fig. 11). The steady photocurrent occurs only at neutral or high pH (where net proton release occurs) and is absent at low pH (where net proton uptake occurs) (compare the upper curves of Figs. 5 and 9).

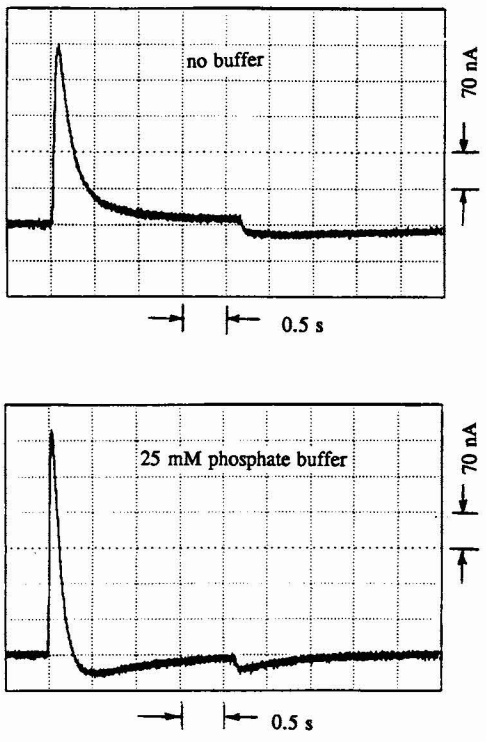

FIGURE 11 Effect of buffer concentration on the time dependence of the photocurrent produced by randomly oriented D96N films. Electrolyte: 100 mM KCl with no buffer at pH ≈7 (*upper curve*) and with 25 mM sodium phosphate buffer at pH 7 (*lower curve*).

DISCUSSION

Miyasaka and Koyama report the transient photocurrent generated by randomly oriented patches of wild-type purple membrane (Miyasaka and Koyama, 1991; Miyasaka and Koyama, 1992; Miyasaka et al., 1992). In a recent paper they compare this transient with transients produced by highly oriented patches of wild-type purple membrane (Koyama et al., 1994). They state that the response mechanism does not involve electron transfer and that the photocurrent is induced electrostatically through charge displacement within the bR molecules. Our model for the photocurrent transient is different; we have described the relevant evidence in the Results section. In the following we explain the shape of the transient they observed and discuss some features of other transients.

Their transient is similar to the lower curve of Fig. 5. We discuss first the sign of the current. The first spike, which occurs when the yellow light is turned on, is cathodic, and the second spike, which occurs when the light is turned off, is anodic. In the Results section we presented evidence that a cathodic current is due to a pH decrease caused by net proton release by bR, and an anodic current is due to a pH increase caused by net proton uptake by bR. Thus in the first spike of Fig. 5, when the light is first turned on, bR releases protons. This agrees with the discussion in the introduction: until bR has had a chance to complete a photocycle, it only releases protons and does not uptake them.

The cycle time of bR is about 10 ms. So, for the first 20 or 30 ms, there is a net release of protons, and the current is cathodic. After that, bR starts to uptake protons, but that uptake is balanced by continued release of protons, so there is only a small net change in proton concentration. Since this change is positive, a cathodic current is still produced. This explains the sign of the first photocurrent spike.

Only the proton concentration at the electrode surface is important. In a film of randomly oriented patches of purple membrane, about half of the patches are oriented with the

periplasmic surface next to the electrode, and these are the patches that release protons to the electrode. The remainder of the patches are oriented with the cytoplasmic surface next to the electrode, and these are the patches that uptake protons from the electrode. The observed current is the sum of a cathodic part due to proton release and an anodic part due to uptake.

When the light is shut off, bR immediately ceases to release protons, but continues to uptake them. This produces an anodic spike for wild-type bR. We have explained the sign of the transient and next will discuss its shape.

The shape and time scale of the photocurrent transient for wild-type bR is almost identical to the current transient that results from a -1 mV step. The evidence given in the results section shows that the light-on current transient is caused by a step increase in proton concentration, which (as in Fig. 7) causes a step increase in the equilibrium potential. Because the interface is in potentiostatic mode, and because only differences in potential are relevant, the increase in the equilibrium point has the same effect as a decrease (of the same magnitude) in the potential applied between the working and reference electrodes. Thus the lower curve in Fig. 5 is the response to a step change in pH or equivalently to a step change in the proton concentration. The shape of this photocurrent transient is due to the motion of supporting ions, in the same way that the shape of a voltage-step-induced transient is.

The more generally shaped transients in the other figures may involve a kind of convolution of the step response with the proton concentration generated by bR. A different limiting case for the generally shaped transient involves mutants such as D96N bR. These have an M-state decay rate so slow that the photocurrent transients can be explained, as in the Results section, and as we discuss briefly in the following.

The light-off transient for D96N bR at pH 7, in the upper curve in Fig. 5, has a decay rate that is much slower than the light-off transient for wild-type bR. The reason is that the observed current transient results from the pH change due to the uptake of protons by bR, which occurs during the M-state decay. For the D96N mutant this decay is slow compared with that for the wild type (Otto et al., 1989; Tittor et al., 1989). The time constant of the light-off current decay for D96N bR at pH 7 is 2 s, which is the same as we observed by measuring the optical absorbance at 412 nm of the same film in the same solution. This decay rate for D96N is faster at acid pH than at normal pH (Miller and Oesterhelt, 1990; Holz et al., 1989; Tittor et al., 1989), as can be seen by comparing the decays of the light-off transients in the upper curves of Figs. 9 and 5. At neutral pH the slow uptake of protons causes a slow change in pH next to the electrode, and this results in a slow decay in the electrochemical current. This explains the light-off transient generated by D96N bR.

The electrostatic charge-displacement model, on the other hand, is not able to explain the almost constant current that occurs in the light-off part of the upper curve in Fig. 5. Thus the pH-change model is in agreement with experiment, and the electrostatic charge-displacement model is not.

SUMMARY AND CONCLUSION

A film of randomly oriented purple-membrane patches on a tin-oxide electrode in an electrolyte, when illuminated with yellow light, produces a transient current. An example is given in the upper left of Fig. 1. The photocurrent is caused by the bR in the film and is not due to the electrode alone.

The bR produces a transient change in pH, which is converted by the electrochemical system into a current transient. This explanation differs from that by Koyama et al. (1994); relevant evidence is given in detail in the Results and Discussion sections. The calibration of the current peak due to a given pH change is given by Figs. 7 and 8. The initial peak of the photocurrent transient is very much larger than the change in constant current produced by a steady-state pH change of the same magnitude. This makes the transient pH measurement highly sensitive.

The measuring technique can be used to study the properties of molecules that can produce a pH change, in particular bR itself. The high sensitivity of the tin-oxide electrode provides a measurable signal from a small quantity of bR.

This work was supported in part by a grant for Cooperation in Applied Science and Technology (CAST) from the National Research Council.

REFERENCES

Balashov, S. P., R. Govindjee, M. Kono, E. Imasheva, E. Lukashev, T. G. Ebrey, R. K. Crouch, D. R. Menick, and Y. Feng. 1993. Effect of the arginine-82 to alanine mutation in bacteriorhodopsin on dark adaptation, proton release, and the photochemical cycle. *Biochemistry*. 32:10331–10343.

Bard, A. J., and L. R. Faulkner. 1980. Electrochemical Methods, Fundamentals and Applications. Ch. 3: Kinetics of Electrode Reactions. John Wiley & Sons, New York. Eqs. (3.3.14) and (3.5.10).

Becher, B., and J. Y. Cassim. 1975. Improved isolation procedures for the purple membrane of Halobacterium halobium. *Prep. Biochem.* 5:161–178.

Butt, H.-J., K. Fendler, E. Bamberg, J. Tittor, and D. Oesterhelt. 1989. Aspartic acids 96 and 85 play a central role in the function of bacteriorhodopsin as a proton pump. *EMBO J.* 8:1657–1663.

Deltombe, E., N. de Zoubov, C. Vanleugenhaghe, and M. Pourbaix. 1966. Tin. *In* Atlas of Electrochemical Equilibria in Aqueous Solutions. Pergamon Press, Elmsford, NY. 475–484.

Dencher, N., and M. Wilms. 1975. Flash photometric experiments on the photochemical cycle of bacteriorhodopsin. *Biophys. Struct. Mechanism* 1:259–271.

Druckmann, S., N. Friedman, J. K. Lanyi, R. Needleman, M. Ottolenghi, and M. Sheves. 1992. The back photoreaction of the M intermediate in the photocycle of bacteriorhodopsin: mechanism and evidence for two M species. *Photochem. Photobiol.* 56:1041–1047.

Ebrey, T. G. 1993. Light energy transduction in bacteriorhodopsin. *In* Thermodynamics of Membrane Receptors and Channels. M. B. Jackson, editor. CRC Press, Boca Raton, FL. 353–387.

Fog, A., and R. P. Buck. 1984. Electronic semiconducting oxides as pH sensors. *Sensors Actuators* 5:137–146.

Galus, Z. 1975. Tin. *In* Encyclopedia of Electrochemistry of the Elements. A. J. Bard, editor. Marcel Dekker, Inc., New York. 223–271.

Garty, H., G. Klemperer, M. Eisenbach, and S. R. Caplan. 1977. The direction of light-induced pH changes in purple membrane suspensions. *FEBS Lett.* 81:238–242.

Groma, G. I., F. Raksi, G. Szabo, and G. Varo. 1988. Picosecond and nanosecond components in bacteriorhodopsin light-induced electric response signal. *Biophys. J.* 54:77–80.

Haronian, D., and A. Lewis. 1991. Elements of a unique bacteriorhodopsin neural network architecture. *Appl. Optics*. 30:597–608.

Holz, M., L. A. Drachev, T. Mogi, H. Otto, A. D. Kaulen, M. P. Heyn, V. P. Skulachev, and H. G. Khorana. 1989. Replacement of aspartic acid-96 by asparagine in bacteriorhodopsin slows both the decay of the M intermediate and the associated proton movement. *Proc. Natl. Acad. Sci. USA*. 86:2167–2171.

Jarzebski, Z. M., and J. P. Marton. 1976. Physical properties of SnO_2 materials. *J. Electrochem. Soc.* 123:199C-205C; 299C-310C; and 333C-346C.

Karvaly, B., and Z. Dancshazy. 1977. Bacteriorhodopsin: a molecular photoelectric regulator. Quenching of photovoltaic effect of bimolecular lipid membranes containing bacteriorhodopsin by blue light. *FEBS Lett.* 76: 36–40.

Kim, H., and H. A. Laitinen. 1975. Photoeffects at polycrystalline tin oxide electrodes. *J. Electrochem. Soc.* 122:53–58.

Kono, M., S. Misra, and T. G. Ebrey. 1993. pH dependence of light-induced proton release by bacteriorhodopsin. *FEBS Lett.* 331:31–34.

Kononenko, A. A., E. P. Lukashev, S. K. Chamorovsky, A. V. Maximychev, S. F. Timashev, L. N. Chekulaeva, A. B. Rubin, and V. Z. Paschenko. 1987. Oriented purple membrane films as a probe for studies of the mechanism of bacteriorhodopsin functioning. II. Photoelectric processes. *Biochim. Biophys. Acta*. 892:56–67.

Koyama, K., N. Yamaguchi, and T. Miyasaka. 1994. Antibody-mediated bacteriorhodopsin orientation for molecular device architectures. *Science*. 265:762–765.

Laitinen, H. A. and T. M. Hseu. 1979. Chemically treated tin oxide electrodes responsive to pH and sulfide. *Anal. Chem.* 51:1550–1552.

Lanyi, J. 1993. Proton translocation mechanism and energetics in the light-driven pump bacteriorhodopsin. *Biochim. Biophys. Acta*. 1183:241–261.

Mathies, R. A., S. W. Lin, J. B. Ames, and W. T. Pollard. 1991. From femtoseconds to biology: mechanism of bacteriorhodopsin's light-driven proton pump. *Ann. Rev. Biophys. Biophys. Chem.* 20:491–518.

McIntosh, A. R., and F. Boucher. 1991. On the action spectrum of the photoelectric transients of bacteriorhodopsin in solid-state films. *Biochim. Biophys. Acta*. 1056:149–158.

Miller, A., and D. Oesterhelt. 1990. Kinetic optimization of bacteriorhodopsin by aspartic acid 96 as an internal proton donor. *Biochim. Biophys. Acta*. 1020:57–64.

Miyasaka, T., and K. Koyama. 1991. Photoelectrochemical behavior of purple membrane Langmuir-Blodgett films at the electrode-electrolyte interface. *Chem. Lett.* 1645–1648.

Miyasaka, T., and K. Koyama. 1992. Rectified photocurrents from purple membrane Langmuir-Blodgett films at the electrode-electrolyte interface. *Thin Solid Films*. 210/211:146–149.

Miyasaka, T., K. Koyama, and I. Itoh. 1992. Quantum conversion and image detection by a bacteriorhodopsin-based artificial photoreceptor. *Science*. 255:342–344.

Oesterhelt, D., and W. Stoeckenius. 1971. Rhodopsin-like proteins from the purple membrane of Halobacterium halobium. *Nature New Biol.* 233: 149–154.

Otto, H., T. Marti, M. Holz, T. Mogi, M. Lindau, H. G. Khorana, and M. P. Heyn. 1989. Aspartic acid-96 is the internal proton donor in the reprotonation of the Schiff base of bacteriorhodopsin. *Proc. Natl. Acad. Sci. USA*. 86:9228–9232.

Oldham, K. B. and J. C. Myland. 1994. Fundamentals of Electrochemical Science. Ch. 5: Electrode Reactions. Academic Press, New York. Equation 5:9:1.

Soppa, J., and D. Oesterhelt. 1989. Bacteriorhodopsin mutants of Halobacterium sp. GRB. I. The 5-bromo-2′-deoxyuridine selection as a method to isolate point mutants in Halobacteria. *J. Biol. Chem.* 264:13043–13048.

Takeuchi, Y., K. Ohno, M. Yoshida, and K. Nagano. 1981. Light-induced proton dissociation and association in bacteriorhodopsin. *Photochem. Photobiol.* 33:587–592.

Tittor, J., C. Soell, D. Oesterhelt, H.-J. Butt., and E. Bamberg. 1989. A defective proton pump, point-mutated bacteriorhodopsin Asp96>Asn is fully reactivated by azide. *EMBO J.* 8:3477–3482.

Varo, G. 1981. Dried oriented purple membrane samples. *Acta Biol. Acad. Sci. Hung.* 32:301–310.

Varo, G., and J. K. Lanyi. 1990. Protonation and deprotonation of the M, N, and O intermediates during the bacteriorhodopsin photocycle. *Biochemistry*. 29:6858–6865.

Zimanyi, L., G. Varo, M. Chang, B. Ni, R. Needleman, and J. K. Lanyi. 1992. Pathways of proton release in the bacteriorhodopsin photocycle. *Biochemistry*. 31:8535–8543.